

This article was downloaded by:

On: 25 January 2011

Access details: *Access Details: Free Access*

Publisher *Taylor & Francis*

Informa Ltd Registered in England and Wales Registered Number: 1072954 Registered office: Mortimer House, 37-41 Mortimer Street, London W1T 3JH, UK



Liquid Crystals

Publication details, including instructions for authors and subscription information:

<http://www.informaworld.com/smpp/title~content=t713926090>

Rotational viscosity and molecular structure of nematic liquid crystals

M. L. Dark^a; M. H. Moore^a; D. K. Shenoy^a; R. Shashidhar^a

^a Center for Bio-Molecular Science and Engineering, Code 6900, Naval Research Laboratory, Washington, DC 20375

To cite this Article Dark, M. L. , Moore, M. H. , Shenoy, D. K. and Shashidhar, R.(2006) 'Rotational viscosity and molecular structure of nematic liquid crystals', *Liquid Crystals*, 33: 1, 67 – 73

To link to this Article: DOI: 10.1080/02678290500450634

URL: <http://dx.doi.org/10.1080/02678290500450634>

PLEASE SCROLL DOWN FOR ARTICLE

Full terms and conditions of use: <http://www.informaworld.com/terms-and-conditions-of-access.pdf>

This article may be used for research, teaching and private study purposes. Any substantial or systematic reproduction, re-distribution, re-selling, loan or sub-licensing, systematic supply or distribution in any form to anyone is expressly forbidden.

The publisher does not give any warranty express or implied or make any representation that the contents will be complete or accurate or up to date. The accuracy of any instructions, formulae and drug doses should be independently verified with primary sources. The publisher shall not be liable for any loss, actions, claims, proceedings, demand or costs or damages whatsoever or howsoever caused arising directly or indirectly in connection with or arising out of the use of this material.

Rotational viscosity and molecular structure of nematic liquid crystals

M. L. DARK, M. H. MOORE, D. K. SHENOY* and R. SHASHIDHAR

Center for Bio-Molecular Science and Engineering, Code 6900, Naval Research Laboratory,
4555 Overlook Avenue SW, Washington, DC 20375, USA

(Received 18 June 2005; accepted 31 August 2005)

An electro-optical technique was used to measure the rotational viscosity of nematic liquid crystals, whose structures were chosen to investigate the effects of linking groups and lateral groups on rotational viscosity. These results are compared with the theory developed by Osipov and Terentjev. It is shown that the theory is useful in predicting rotational viscosity for specific molecular structures. The agreement between theory and experiment is found to be good for all the liquid crystals studied.

1. Introduction

Rotational viscosity is an important physical property of liquid crystals. In some electro-optical devices using liquid crystals in the nematic phase, the response time is proportional to the rotational viscosity (γ_1). Rotational viscosity characterizes friction between liquid crystal (LC) directors during molecular rotations, and its magnitude depends on temperature, intermolecular interactions, and the molecular structure. The relationship between structure and rotational viscosity is particularly interesting because by modifying a liquid crystal structure, one could tailor a molecule in order to decrease viscosity. There have been many experimental studies of the rotational viscosity of liquid crystals [1–7], some of which have focused on the relationship between rotational viscosity and structure [8–11].

Microscopic theories of rotational viscosity were developed by Diogo and Martins (1981), Kuzuu and Doi (1983), and Osipov and Terentjev (1989) [10–12]. The theory of rotational viscosity of Diogo and Martins is interesting from a historical approach, but difficult to apply to experimental results because of the many free parameters. Kuzuu–Doi (KD) considered the stress tensor to be an average of the microscopic stress tensor. Considering the asymmetric part by using a perturbation method and solving the kinetic equations, Osipov–Terentjev (OT) derived an expression for the microscopic stress tensor for a nematic based on molecular moments of inertia and intermolecular interaction potential. This was an attempt to improve upon the KD theory. Further

considerations of these theories have been performed recently [13, 14]. The OT theory also provides insight into the relationship between rotational viscosity and molecular structure and its dimensions. The purpose of this work is to determine the effect of molecular structure on the rotational viscosity, and in particular the influence of the molecular length-to-breadth ratio, on rotational viscosity. A systematic study of this type has not been reported previously. By changing the linking group and lateral groups, we can compare the experimentally measured rotational viscosity with predictions of the OT theory.

2. Experimental

Several methods have been used to measure the rotational viscosity of liquid crystals [1–7]. Rotational viscosity can be measured directly using a sample suspended in a rotating magnetic field [1]; it can also be determined by a relaxation method, by measuring certain physical properties of the liquid crystal [7]. We used the latter method, in which the time decay of the optical phase retardation of the LC cell is measured. A small voltage is applied to a LC cell so that the nematic directors are deformed by a small angle. At time $t=0$, this voltage is removed and the molecules relax with relaxation time τ_0 to the equilibrium state, which is a parallel alignment. For a LC slab of thickness d , τ_0 is related to the materials parameters and cell thickness by:

$$\gamma_1 = \frac{\tau_0 k_{11} \pi^2}{d^2} \quad (1)$$

where k_{11} is the splay elastic coefficient and γ_1 is the rotational viscosity of the liquid crystal. The splay

*Corresponding author. Email: dshenoy@cbmse.nrl.navy.mil

elastic coefficient depends on the threshold voltage (V_{th}) and is obtained from a Frédricks transition experiment through the relation:

$$k_{11} = \left(\frac{V_{th}}{\pi} \right)^2 \Delta \varepsilon \varepsilon_0 \quad (2)$$

where $\Delta \varepsilon (= \varepsilon_{||} - \varepsilon_{\perp})$ is the dielectric anisotropy of the LC. Thus, by measuring the following physical properties of each liquid crystal as functions of temperature: τ_0 , V_{th} , and $\Delta \varepsilon$, the splay elastic constant may be obtained.

In this work, we studied four different nematic LCs whose molecular structure was systematically varied. The well known material (5CB) 4-*n*-pentyl-4'-cyanobiphenyl was chosen as standard. Using this LC, our experimental results could be compared with literature results to ascertain the accuracy of our measurements. To investigate the effect of the linking group on γ_1 , we synthesized a material, 4-cyanobiphenyl 4-pentylbenzoate (CBP5), which resembles 5CB, but has an ester group between the phenyl rings. To investigate the effect of lateral groups, we studied 4-octylphenyl 2-chloro-4 (4-heptylbenzoyloxy)benzoate (8PCB) and 4-pentylphenyl 2-chloro-4 (4-pentylbenzoyloxy)benzoate (5PCB), two commercially available liquid crystals with differing chain lengths. Their structures and nematic-isotropic transition temperatures are shown in table 1.

2.1. Relaxation time constant

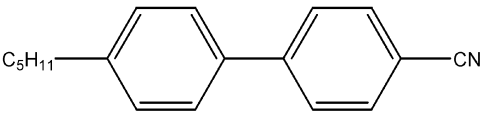
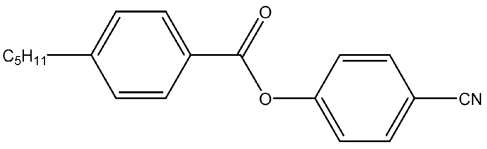
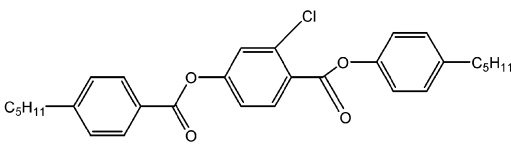
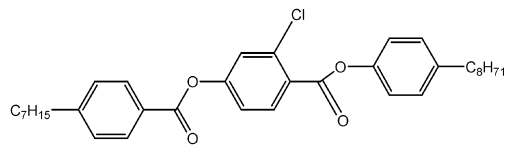
By measuring the transmitted light intensity through a planar aligned LC cell, we can obtain the optical phase as a function of time. By assuming that the LC directors are deformed by the applied voltage by a small angle, the decay time can be approximated as in the following equation [7]:

$$\delta(t) \cong \delta_0 \exp(-2t/\tau_0) \quad (3)$$

where δ_0 is the total phase change of the LC cell under a bias voltage V_B . In the case where δ_0 is close to $N\pi$ (N =integer), then the expression for $\delta(t)$ becomes $\delta_0 \exp(-4t/\tau_0)$ [15]. By plotting $\ln[\delta_0/\delta(t)]$ versus time, we confirm that the phase $\delta(t)$ is an exponential function as expected from equation(3). The slope of this linear plot is $2/\tau_0$, which thus yields the relaxation time.

Two experiments were performed in order to obtain the relaxation time. In the first experiment (i), we measured the transmitted laser light intensity as a function of voltage. The experimental set-up is shown in figure 1. A He-Ne laser ($\lambda=632.8$ nm, Melles Griot) provides the incident laser light which is directed onto a

Table 1. Structures and N-I transition temperature of the liquid crystal materials studied.

Compound ($T_{NI}/^{\circ}\text{C}$)	Structure
5CB (35.4)	
CBP5 (57)	
5PCB (123)	
8PCB (105)	

LC cell placed between two crossed linear polarizers. A Glan Thomson polarizer is used to linearly polarize the laser light at 45° to the horizontal. The temperature control of the LC cell is provided by an INSTEC temperature controller (Instec, Inc). A voltage is applied to the cell via an LCR meter (HP-4284A). The LC cell capacitance is measured using the HP LCR meter and the transmitted light is measured using a photodiode (Graseby Optronics, model 264) calibrated at 632.8 nm. The glass plates used for fabricating the cells (EHC Industries, Japan) are coated with a polyimide layer for planar alignment, with an electrode surface area of 1 cm^2 . Glass rod spacers determine the cell thickness. Using an interferometric technique, a LC cell containing 5CB was measured to have a thickness of $d=9.9\ \mu\text{m}$. Figure 2 shows the transmission of the laser light through the 5CB sample cell as a function of voltage at $T=22^{\circ}\text{C}$. The total optical phase retardation is determined to be $\Delta_{tot}=6.09\ \pi$ by counting the interference fringes. The optical birefringence is determined

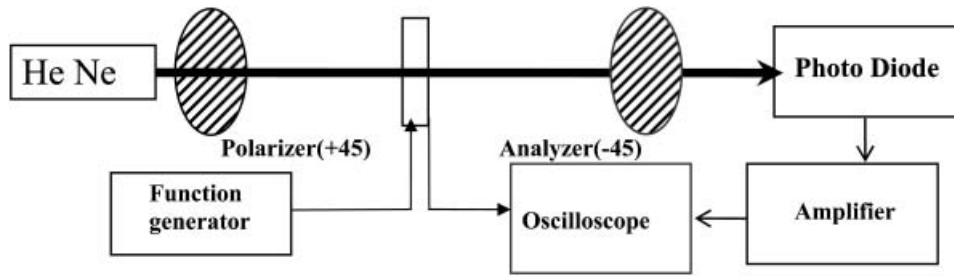


Figure 1. Schematic of experimental set-up. Polarizers are oriented with the axis 45° to the horizontal.

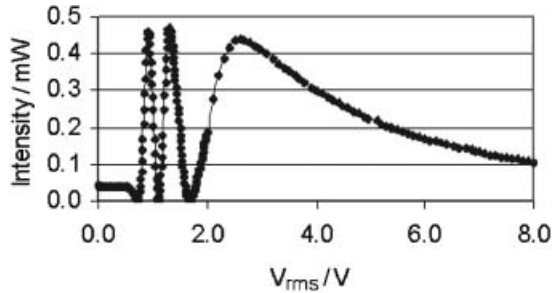


Figure 2. Transmitted intensity of 5CB at $T=21.8^\circ\text{C}$. Cell thickness is $9.9\ \mu\text{m}$; first maximum occurs at $V=0.90\ V_{\text{rms}}$.

from the retardation $\Delta n = \Delta_{\text{tot}} \lambda / 2\pi d$, and for 5CB is calculated to be 0.195 at 22°C .

In the second experiment (ii), a small bias voltage is applied to the LC cell, corresponding with the first maximum (or minimum) in transmission (as given in the data shown in figure 2). The photodiode output is sent to an amplifier and then to an oscilloscope. Figure 3 shows the transmitted laser light intensity through the LC cell containing 5CB, as a voltage output as a function of time. When the voltage ($V_b = 0.90\ V_{\text{rms}}$) is removed, as expected the optical transmission decreases then increases slightly. The phase change $\delta(t)$ as a

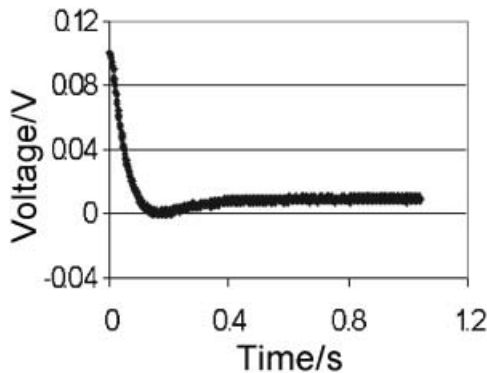


Figure 3. Time-dependent intensity of 5CB. The total phase change is $\delta_0 = 1.09\pi$ for a bias voltage of $V_b = 0.90\ V_{\text{rms}}$.

function of time can be calculated from the time-dependent intensity, $I(t)$, using the following equation:

$$I(t) = I_0 \sin^2 \{(\Delta_{\text{tot}} - \delta(t))/2\} \quad (4)$$

where I_0 is the maximum intensity change. Once $\delta(t)$ is determined, we plot $\ln[\delta_0/\delta(t)]$ versus time as in figure 4, and obtain the slope of the linear plot, equation (3). The relaxation time is ascertained from the slope as described previously. The standard deviation of the relaxation time measurement is estimated to be $\pm 5\ \text{ms}$.

2.2. Fréedericks transition voltage

The Fréedericks transition voltage is needed to determine the splay elastic coefficient, and is obtained from the capacitance versus voltage measurement described in the previous section. For the materials studied with positive dielectric anisotropy materials ($\Delta\epsilon > 0$), the capacitance of the material begins to increase quickly once it reaches the transition voltage.

2.3. Splay elastic and dielectric constants

To determine the rotational viscosity γ_1 we must know the splay elastic constant k_{11} as seen from equation (2). The Fréedericks transition voltage is obtained experimentally as described in §2.2. Dielectric constants were

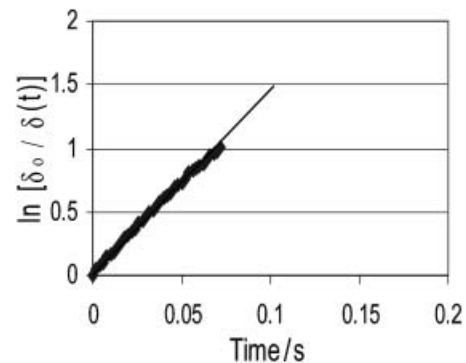


Figure 4. $\ln[\delta_0/\delta(t)]$ versus time for 5CB. The value of the slope is $14.6\ \text{s}^{-1}$, giving a relaxation time of $\tau_0 = 270\ \text{ms}$.

determined from capacitance measurements of planar and homeotropically aligned cells. A HP LCR meter was used to measure capacitance at a frequency of 1 kHz.

The capacitance of the empty cell was measured before filling it with liquid crystal. Capacitance values were normalized to the empty cell capacitance $C_0 = \epsilon_0 A / d$, where the area of the electrode is $A = 1.0 \text{ cm}^2$. After filling with liquid crystal, the capacitance of the cell in planar geometry was measured at a voltage below the Fréedericks threshold, and at a voltage approximately ten times larger than the threshold for homeotropic alignment. For a liquid crystal with positive dielectric anisotropy, the planar cell yields ϵ_{\perp} and the homeotropic cell ϵ_{\parallel} . Measurements of the dielectric anisotropy of 5CB were in close agreement with those reported in the literature [16]. Having ascertained the accuracy of our set-up using 5CB as the standard LC material, we performed the experiments on the other three materials (CBP5, 5PCB and 8PCB) to obtain the rotational viscosities as a function of temperature.

3. Results

Fréedericks transition experiments, as well as the relaxation time and dielectric anisotropy measurements, were performed using the four LC materials shown in table 1, in order to determine the rotational viscosity as a function of temperature. Table 2 summarizes the physical properties obtained for each material at a similar reduced temperature $T/T_{NI} = 0.965$. Measured relaxation times are shown for all four samples in figure 5. The relaxation time of the CBP5 liquid crystal material is lower than that of nematic 5CB. Among the materials with lateral groups, the 8PCB sample, having the longer chain length, shows a higher relaxation times (almost by a factor of 2). The Fréedericks threshold voltages are shown for all the four samples in figure 6. 5CB and CBP5 have similar threshold voltages, which are much smaller than the PCB materials. This is evidently due to the higher dipole moment of the cyano group. Figure 7 shows birefringence of each material versus temperature; 5CB has the highest birefringence. The ‘three-ring’ LC materials show the lowest birefringence values.

Table 2. Physical properties of samples at $T/T_{NI} \approx 0.965$.

Compound	$\gamma_1 / \text{Pa s}$	$\Delta\epsilon$	$V_{th} \text{ (rms)}$	$k_{11} / 10^{-12} \text{ N}$	Δn
5CB	0.087	11.0	0.70	4.78	0.19
CBP5	0.067	19.8	0.51	4.53	0.15
5PCB	0.047	2.7	1.72	7.10	0.12
8PCB	0.051	4.9	1.88	4.97	0.10

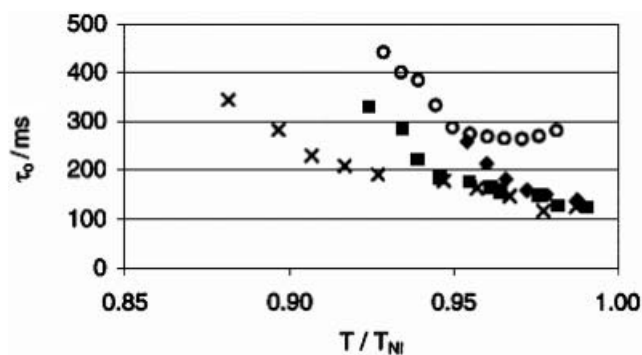


Figure 5. Relaxation time measurements versus temperature. The data symbols are as follows: 5CB (\diamond), CBP5 (\blacksquare), 5PCB (\times), and 8PCB (\circ).

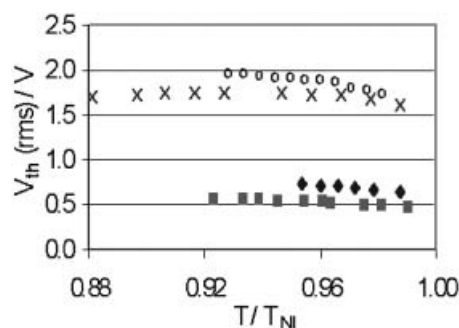


Figure 6. Fréedericks threshold voltage measurements versus temperature. The data symbols are as follows: 5CB (\diamond), CBP5 (\blacksquare), 5PCB (\times), and 8PCB (\circ).

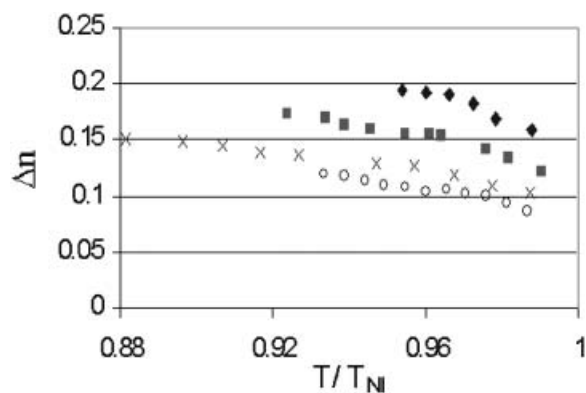


Figure 7. Variation of birefringence of LC materials with temperature. The data symbols are as follow: 5CB (\diamond), CBP5 (\blacksquare), 5PCB (\times), and 8PCB (\circ).

Our dielectric anisotropy measurements for 5CB agree with published results [16]. Figures 8–10 show dielectric anisotropy as a function of temperature for the other three materials. As expected, CBP5 shows a large value of dielectric anisotropy (figure 8). The ‘three-ring’ materials (5PCB, 8PCB) show lower dielectric constants, because they have no terminal cyano group.

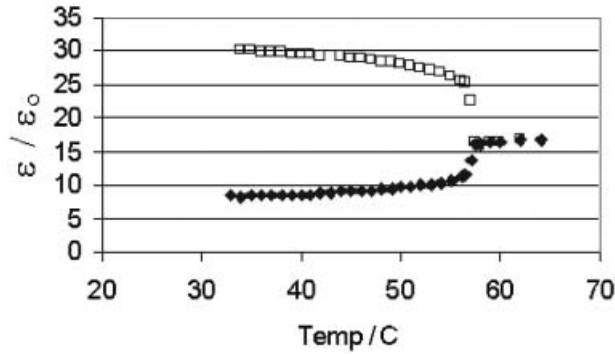


Figure 8. Dielectric constant of CBP5 measured at a sine wave frequency of 1 kHz. Open squares (\square) represent ϵ_{11} and filled diamonds (\blacklozenge) ϵ_{\perp} .

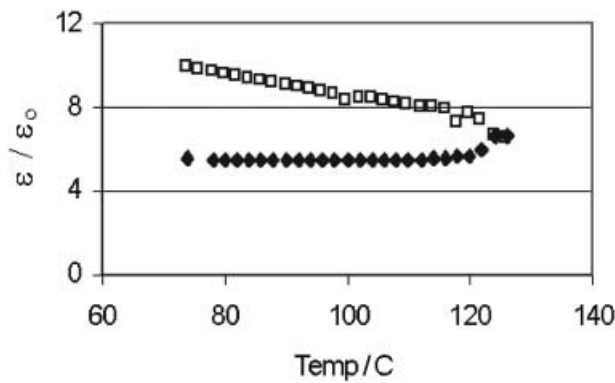


Figure 9. Dielectric constant of 5PCB measured at a sine wave frequency of 1 kHz. Symbols are the same as in figure 8.

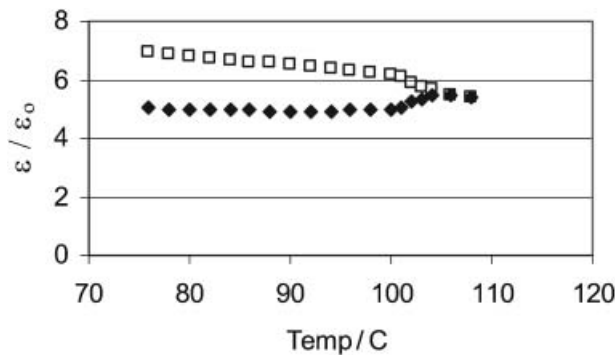


Figure 10. Dielectric constant of 8PCB measured at a sine wave frequency of 1 kHz. Symbols are the same as in figure 8.

By plotting $\ln[\delta_o/\delta(t)]$ versus time in figure 4 and equation (3), we determine the relaxation time for 5CB at $T=22^\circ\text{C}$ to be 270 ms. The Fréedericks transition voltage is $0.70 V_{\text{rms}}$. For 5CB at $T=22^\circ\text{C}$, the dielectric constants are $\epsilon_{\perp}=6.2$ and $\epsilon_{11}=17.6$, giving a dielectric anisotropy of $\Delta\epsilon=11.4$. Using equation (2) to calculate the splay elastic constant, we obtain $k_{11}=5.0 \times 10^{-12} \text{ N}$. From such measurements, the rotational viscosity of

5CB, CBP5, 5PCB and 8PCB have been plotted as functions of reduced temperature in figures 11–14. The data for 5CB agree well with reported measurements, which were obtained using two different methods [1, 7]. In all cases, the solid line is the theoretically predicted rotational viscosity from Osipov and Terentjev [12]. We

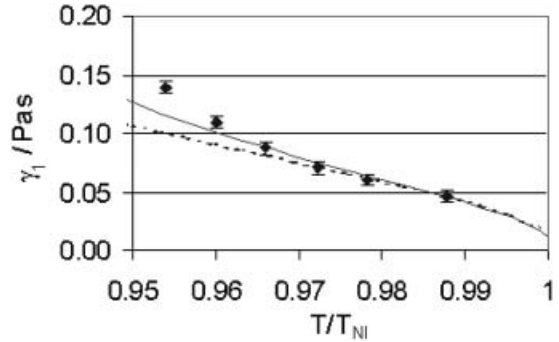


Figure 11. Rotational viscosity of 5CB as a function of temperature. Experimental data are represented by (\blacklozenge). The solid line represents the prediction from OT theory; the dashed line represents that using the length-to-breadth ratio.

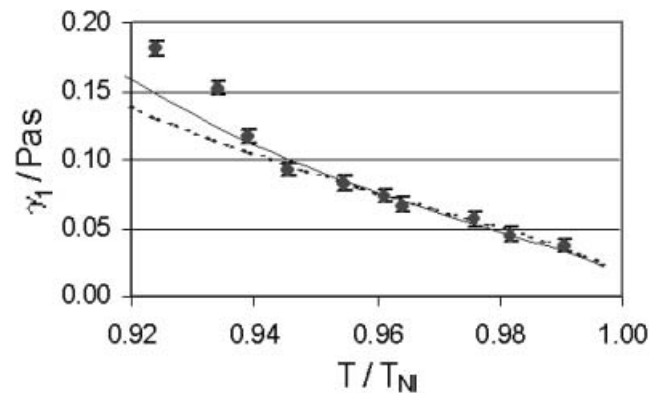


Figure 12. Rotational viscosity of CBP5 as a function of temperature. Solid and dashed lines, as for figure 11.

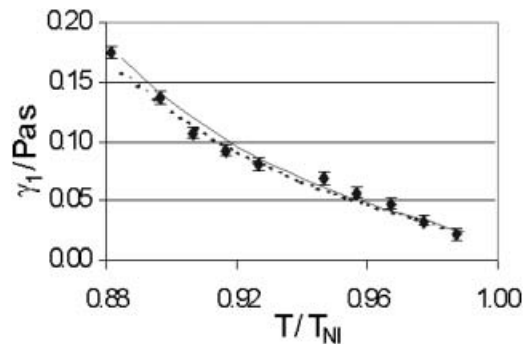


Figure 13. Rotational viscosity of 5PCB as a function of temperature. Solid and dashed lines, as for figure 11.

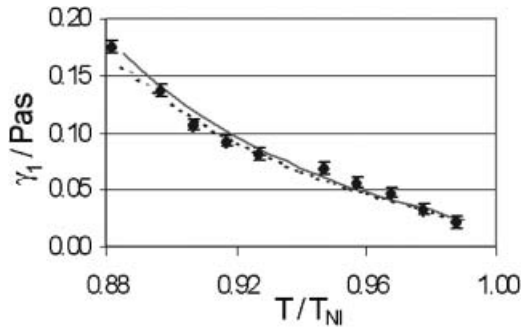


Figure 14. Rotational velocity of 8PCB as a function of temperature. Solid and dashed lines, as for figure 11.

shall discuss this aspect in the next section. It should be mentioned that CBP5 (figure 12) shows higher values of γ_1 than predicted, particularly at temperatures $T/T_{NI} < 0.94$. The higher viscosity could be attributed to the sample approaching the crystallization temperature.

4. Discussion

According to the theory of Osipov and Terentjev [12], assuming rod-like molecules, the rotational viscosity is given by

$$\gamma_1(T) \cong \frac{1}{6} c \lambda (J/kT)^{\frac{1}{2}} \exp\left(\frac{J}{kT}\right)^2 \quad (5)$$

where J is the mean-field coupling constant, c is number density of molecules and λ is the microscopic friction coefficient. The expression for the friction coefficient is as follows:

$$\lambda \cong 100(1-\phi)c^2w^6\left(\frac{w}{l}\right)^2\frac{(kT)^5}{G^3}\left(I_{\perp}/kT\right)^{\frac{1}{2}}\exp\left(3\frac{G+I_o}{kT}\right) \quad (6)$$

where ϕ is the volume fraction of molecules (0.5–0.6 for dense molecular liquids) and I_{\perp} and I_o are inertia tensors. The isotropic intermolecular interaction energy G is approximately one-third the activation energy; $E_1 = 3G$. The expression for γ_1 can be rewritten with three fitting parameters as follows [8]:

$$\gamma_1 = g_o (T/T_{NI})^4 (E_1/kT_{NI})^{-3} (J_o S/kT_{NI})^{\frac{1}{2}} \exp\left(\frac{E_1 + J_o S}{kT}\right) \quad (7)$$

where S is the order parameter of the nematic, g_o is a constant, and $J_o = BkT_{NI}$. Here one must treat g_o , J_o and E_1 as free parameters of the fit. The order parameter as a function of temperature, $S(T)$, is obtained from the experimentally determined birefringence of each sample [7].

In an attempt to reduce the number of fitting parameters to two, we used the software package HyperChem (Hypercube) to calculate the length-to-breadth

Table 3. Length-to-breadth ratios as determined by HyperChem.

Compound	L/w
5CB	3.33
CBP5	3.63
5PCB	5.33
8PCB	6.01

ratio (L/w) of the molecule. Table 3 lists the length-to-breadth ratios for each sample. Thus, the proportionality constant g_o can be a fixed parameter, and only J_o and E_1 are free parameters. The dashed line in figures 11–14 is the theoretical prediction using two parameters. Hence, we are able effectively to predict rotational viscosity as a function of temperature using only two fitting parameters.

The fitting parameters are listed in table 4. The values of activation energies (E_1) are in the range 160–410 meV, which are similar to those found for other nematics [7]. The value of J_o should be approximately $4.5kT_{NI}$, calculated from mean field theory [17]. Our values are in the range 2.0–4.3 kT_{NI} . Although lower than expected, they are reasonable values considering the complicated interactions involved in the theory. Because the two terms J_o and E_1 are connected via the exponential term, $\exp[(E_1 + J_o S)/kT]$, a change in one can be compensated for by changing the other. However, by going to a two-parameter fit, we should be able to increase the accuracy in determining J_o and E_1 from γ_1 .

As the OT theory predicts in equations (5) and (6), rotational viscosity is inversely proportional to (L/w) [2]. The samples we used have similar widths, because the cores are composed of phenyl rings. In considering length-to-breadth ratios of CBP5 and 5CB, we would expect CBP5 to have a lower viscosity than 5CB by approximately 84%. Our experimental data show this result, as the rotational viscosity values are

Table 4. Fitting parameters used for fitting Osipov–Terentjev theory to γ_1 data.

Compound	$g_o/\text{Pa s}$	E_1/meV	J_o/kT_{NI}
5CB	9.0×10^{-5}	284	4.29
CBP5	8.9×10^{-5}	292	3.54
5PCB	1.1×10^{-4}	325	2.04
8PCB	1.5×10^{-4}	329	2.09
Using L/w ratio (table 3)			
5CB		163	4.29
CBP5		222	3.54
5PCB		399	2.04
8PCB		408	2.09

γ_1 (CBP5)=0.8 γ_1 (5CB). By comparing length-to-breadth ratios of 5CB and 5PCB, one expects γ_1 (5PCB) to decrease to approximately 0.4 γ_1 (5CB). The experimental results show γ_1 of 5PCB to be 0.5 of the 5CB viscosity.

The second pair of molecules, however, does not behave as predicted. They show similar values of rotational viscosity, and at lower temperatures, 8PCB shows a higher viscosity. This could suggest that a sample with longer carbon chains is less rigid. Thus, a rigid rod-based model may need additional considerations for complete prediction of its behavior. Diogo and Martins have also observed increasing rotational viscosity with increasing chain length in di-*n*-alkyloxy-azoxybenzenes [10]. Another study of molecular structure and rotational viscosity determined that molecules with longer alkyl chains show increasing viscosity [9]. The authors also suggest that molecules with a higher number of phenyl rings show increasing viscosity, but this does not agree with our data. However, they also state that their empirical rules can be superseded by a variety of other effects within the liquid crystal.

5. Conclusion

The OT theory dependence on molecular dimensions was compared with the experimental measurements of rotational viscosity on four different liquid crystal materials with differing molecular structures. The length-to-breadth ratio is a useful parameter for prediction of differences between the rotational viscosities of related materials. It can also be used to predict trends of rotational viscosities based on molecular structure, and therefore as a guide to the synthesis of liquid crystal materials with desirable physical properties.

Acknowledgements

The authors wish to thank Dr M. Spector, Dr J. Selinger, and B. Weslowski for helpful discussions. We also wish to thank Dr J. Naciri for suggestions concerning the synthesis of CBP5. M. L. D. wishes to acknowledge the NRC for a postdoctoral fellowship.

References

- [1] H. Knepe, F. Schneider, N.K. Sharma. *J. chem. Phys.*, **77**, 3203 (1982).
- [2] P.R. Gerber. *Appl. Phys.*, **A26**, 139 (1981).
- [3] P. Cladis. *Phys. Rev. Lett.*, **28**, 1629 (1972).
- [4] H. Schad, H.R. Zeller. *Phys. Rev. A*, **26**, 2940 (1982).
- [5] E.E. Pashkovsky, T.G. Litvina. *Macromolecules*, **28**, 1818 (1995).
- [6] G. Christoph, W. Stille, G. Strobl. *J. Chem. Phys.*, **99**, 3075 (1993).
- [7] S.T. Wu, C.S. Wu. *Phys. Rev. A*, **42**, 2219 (1990).
- [8] L. Pohl, U. Finkenzeller. In *Liquid Crystals: Applications and Uses*, Vol. I, B. Bahadur (Ed.), pp. 163–165, World Scientific, River Edge, NJ (1995).
- [9] H. Knepe, F. Schneider. In *Handbook of Liquid Crystals*, Vol. 2A, D. Demus, J. Goodby, G.W. Gray, H-W. Spiess, V. Vill (Eds), pp. 160–163, Wiley-VCH, New York (1998).
- [10] A.C. Diogo, A.F. Martins. *Mol. Cryst. Liq. Cryst.*, **66**, 133 (1981).
- [11] N. Kuzuu, M. Doi. *J. Phys. Soc. Jpn.*, **52**, 3486 (1983).
- [12] M.A. Osipov, E.M. Terentjev. *Z. Naturforsch.*, **A44**, 785 (1989).
- [13] A. Chrzanowska, K. Sokalski. *Phys. Rev. E*, **52**, 5228 (1995).
- [14] J. Janik, J.K. Moscicki, K. Czuprynski, R. Dabrowski. *Phys. Rev. E*, **58**, 3251 (1998).
- [15] S.T. Wu. *J. Appl. Phys.*, **60**, 1836 (1986).
- [16] B.R. Ratna, R. Shashidhar. *Pramana*, **6**, 278 (1976).
- [17] M.J. Bradshaw, D.G. McDonnell, E.P. Raynes. *Mol. Cryst. Liq. Cryst.*, **70**, 289 (1981).